J. Dairy Sci. 108:5628–5640
https://doi.org/10.3168/jds.2025-26415

Evaluating secondary structure changes in beta-lactoglobulin induced by supercritical CO_2 treatment

Rahul Venkatram,[1] Silvia de Lamo Castellvi,[1,2] Luis Rodriguez-Saona,[1] and Rafael Jiménez-Flores[1]*
[1]Department of Food Science and Technology, The Ohio State University, Columbus, OH 43210
[2]Departament D'Enginyeria Química, Universitat Rovira I Virgili, Campus Sescelades, Tarragona, Spain 43007

ABSTRACT

The focus of this research was to evaluate changes in the secondary structure of β-LG induced by supercritical CO_2 ($ScCO_2$) treatment of whole milk powder (WMP). Processing conditions of 63°C/200 bar and 75°C/300 bar were chosen for further investigation because they produced the highest reduction in antigenicity, 42.9% ± 2.83% (±SD) at 63°C/200 bar and 54.75% ± 2.43% at 75°C/300 bar, respectively, via sandwich ELISA. Orbitrap fusion liquid chromatography-MS/MS detected the presence of capric acid under processing conditions of 63°C/200 bar and lactose molecules at 75°C/300 bar, and these post translational modifications were established to be unique to $ScCO_2$ processing. The β-LG was isolated from reconstituted WMP via isoelectric precipitation and membrane filtration, and secondary structure analysis was conducted via UV-absorption, intrinsic and extrinsic, circular dichroism, and Fourier-transform mid infrared spectroscopy. Results indicated the unfolding of the β-LG molecule, with exposure of Trp residuals to the exterior and an increase in surface hydrophobicity of the protein molecule. Circular dichroism spectroscopy results highlighted an increase in α-helices and random coils with a reduction in β-sheets characteristic to β-LG and thus highlighting significant changes in the secondary structure of the protein. Glycoprotein formation and caprylation had the most significant effects on the amide I and II regions of β-LG, indicative of post-translational modifications and were found to be unique to $ScCO_2$ processing.

Key words: supercritical CO_2, beta-lactoglobulin, fluorescence spectroscopy, circular dichroism, Fourier-transform mid infrared spectroscopy

INTRODUCTION

Cow milk is the most frequently encountered dietary allergen in early infancy when the immune system is immature and susceptible to sensitization from environmental allergens (Crittenden and Bennett, 2005). One of the most prevalent allergens in cow milk is believed to be β-LG, although caseins have also been known to induce immunological responses with a significantly lower prevalence (Villa et al., 2018). The most common approach to tackle allergenicity is high heat treatment, which is known to produce severe protein denaturation with a potential loss in functionality and impairment of sensory attributes (Achouri and Boye, 2013). To overcome these problems, it is imperative to explore other novel processing methods to produce hypoallergenic products.

The usage of supercritical fluid (**SCF**) technology has been increasing tremendously over the years, with a myriad of applications in the food industry. The dairy industry also has been implementing SCF as a potential processing method for a number of applications, such as fat extraction and fractionation, milk pasteurization, and microbial inactivation (Singh et al., 2018). Bonnaillie and Tomasula (2012) and Yver et al. (2011) developed a pilot scale process to fractionate whey proteins from whey protein isolate (**WPI**) using $ScCO_2$. Xu et al. (2011) reported an increase in particle size and turbidity of WPI solutions upon $ScCO_2$ treatment at 60°C owing to protein unfolding and aggregation. Fourier-transform mid infrared (**FT-MIR**) spectroscopy results were instrumental in establishing that the secondary structure of WPI was characterized with a decrease in α-helix content and increase in β-sheets (Xu et al., 2011). During the SCF process, carbonic acid is formed within the extraction vessel, triggering a binding between milk proteins and calcium ions, disrupting the stability of casein micelles, which may be beneficial in cheesemaking (Amaral et al., 2017). A study by Garcia-Cano et al. (2021) observed a 50% reduction in the antigenicity of β-LG via $ScCO_2$ treatment at 75°C/250 bar along with a 25% lower inflammatory response in Caco-2 cells. The primary mechanism

Received February 3, 2025.
Accepted March 11, 2025.
*Corresponding author: jimenez-flores.1@osu.edu

The list of standard abbreviations for JDS is available at adsa.org/jds-abbreviations-25. Nonstandard abbreviations are available in the Notes.

identified in this study was lactosylation. In our previous report (Venkatram et al., 2024), we evaluated the effect of $ScCO_2$ treatment on the antigenic response of β-LG in whole milk powder (**WMP**) and observed a reduction in antibody recognition (antigenicity) via ELISA as a function of lactosylation and caprylation, which were found to be unique to this processing condition. Our results also indicated small changes in functionality, which is key for dairy applications.

The objective of this study was to evaluate changes in the secondary structure of β-LG as a function of $ScCO_2$ processing, which led to a reduction in the antigenicity of the protein via caprylation and lactosylation as 2 unique identified pathways. Secondary structure of proteins plays an instrumental role in antigen-antibody recognition (Pedroza-Escobar et al., 2023), and the aim of this study was to determine changes in the secondary structure as a function of antigenicity. For the purpose of this study, we compare β-LG isolated from WMP to that under $ScCO_2$ conditions. A thermal control has also been included to understand the role of heat in the presence and absence of hydrophobic $ScCO_2$, and the role it plays in secondary structure modification. We hypothesize that $ScCO_2$ processing would impart a unique denaturation mechanism or conformational change to β-LG, different from dry heating, which is also known to produce conformational changes in proteins. The inherent hydrophobicity of $ScCO_2$ would provide a conducive medium to trigger irreversible folding of the β-LG molecule, exposing these hydrophobic domains that could potentially instigate interactions with other components present in the matrix.

MATERIALS AND METHODS

Supercritical CO_2 Processing

Whole milk powder was processed using $ScCO_2$, as previously described by Venkatram et al. (2024). Processing conditions of 63°C/200 bar and 75°C/300 bar were chosen for further investigation in this study owing to the highest reduction of antigenicity and identification of 2 unique pathways to reduce antigenicity of β-LG via caprylation at 63°C/200 bar and lactosylation at 75°C/300 bar.

Isolation of β-LG from WMP

The β-LG was isolated from WMP using the method suggested by Fox et al. (1967). This method mainly relies on the resistance of β-LG toward precipitation in the presence of trichloroacetic acid. Whole milk powder was first prepared as a 10% wt/vol suspension, as previously described in Venkatram et al. (2024). After overnight hydration, this suspension was heated to 37°C in a water bath, after which its pH was reduced to 4.6 using 6 M HCl (Thermo Fisher Scientific, Waltham, MA) with continuous agitation. The pH was monitored using a SevenExcellence pH meter (Mettler Toledo, Columbus, OH) before the addition of 6M HCl. Then, 150 mL of the WMP suspension was acid treated and upon observable precipitation at pH 4.6, was then transferred to 50 mL graduated centrifugal tubes and centrifuged at 4,500 × *g* for 30 min at room temperature to eliminate casein precipitates. The supernatant was then collected, pH readjusted to that of the original suspension and combined with an equal volume of 6% tricholoroacetic acid solution (Sigma Aldrich, St. Louis, MO), and the mixture was allowed to react at room temperature for a total duration of 30 min. The mixture was then transferred to 50 mL centrifugal tubes following centrifugation at 4,500 × *g* for 30 min at room temperature. The supernatant was collected and filtered using 10 kDa Amicon Ultra Centrifugal Filters (Merck Millipore) to remove any unreacted chloride ions. The retentate was then dispensed into a dialysis tubing cellulose membrane (molecular weight cutoff: 14 kDa, Sigma Aldrich), 12 cm in length, and this solution was dialyzed against distilled water at 4°C for 24 h with water changes every 4 h. This process was allowed to continue until a negative chloride ion test was obtained using a chloride ion reflectometric test (Millipore Sigma). After completion of dialysis, the solution was concentrated using Vacufuge plus (Eppendorf, Hamburg, Germany) to yield a final concentration of 1 mg/mL determined using a Micro Bicinchoninic Acid Assay Kit (Thermo Fisher).

UV-Absorption Spectrum Analysis

The UV-absorption spectra of β-LG isolated from WMP was analyzed using a SpectraMax M2 Absorbance and Fluorescence Microplate reader (Molecular Devices, San Jose, CA). Samples at a concentration of 1 mg/mL were homogenized and dispensed as aliquots of 250 µL on Nunc 96-well UV Transparent Microplates (Thermo Fisher Scientific). Samples were read at wavelengths between 270 and 400 nm with increments of 2 nm. The spectral analysis was performed at 25 ± 1°C. Each sample was analyzed in triplicate.

Intrinsic Fluorescence Spectrum Analysis

The intrinsic fluorescence of β-LG, which is due to the natural fluorescence of aromatic side chains in its AA composition (Wang et al., 2015b), was evaluated using a SpectraMax M2 Absorbance and Fluorescence Microplate reader (Molecular Devices) through endogenous fluorescence spectroscopy. Samples at a concentration of

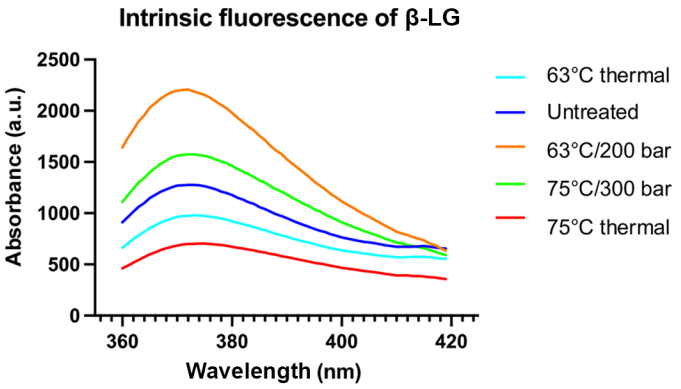

Figure 1. Intrinsic fluorescence of β-LG isolated from whole milk powder under varied supercritical and thermal treatment conditions. a.u. = absorbance unit.

Table 1. Purity of β-LG isolated from reconstituted whole milk powder processed under thermal and supercritical CO_2 conditions[1]

Sample	Protein content (BSA standard [μg/mL])	Protein content (β-LG standard [μg/mL])	β-LG purity (%)
Untreated β-LG	17.24 ± 0.18[a]	16.74 ± 0.09[a]	97.10 ± 0.21[a]
63°C/200 bar	17.72 ± 0.23[a]	17.07 ± 0.28[a]	96.33 ± 0.07[a]
63°C thermal	17.41 ± 0.62[a]	16.93 ± 0.12[a]	97.30 ± 0.42[a]
75°C/300 bar	17.16 ± 0.11[b]	16.35 ± 0.33[b]	95.28± 0.21[b]
75°C thermal	17.42 ± 0.08[a]	17.10 ± 0.74[b]	98.16 ± 0.67[a]

[a,b]Means not sharing a common superscript within a column are different ($P < 0.05$).

[1]Mean values of protein content of β-LG isolated from reconstituted WMP via Bradford assay and purity before and after heat and $ScCO_2$ treatment (±SD). Values are an average of triplicate treatment and triplicate analysis.

1 mg/mL were homogenized and dispensed as aliquots of 250 μL on Nunc 96-well UV Transparent Microplates (Thermo Fisher Scientific). Samples were excited at a wavelength of 280 nm, and the emission was recorded between wavelengths of 360 and 420 nm with increments of 2 nm. The spectral analysis was performed at 25 ± 1°C. Sample analysis was performed in triplicate.

Extrinsic Fluorescence Spectrum Analysis

The extrinsic fluorescence of β-LG, which is caused by an added fluorescent probe, was determined using 8-anilino-1-naphthalenesulfonic acid (**ANS**), as previously described by Meng et al. (2017). First, 20 μL of 0.05 M ANS (0.015 g ANS in 0.05 M PBS, pH 6.8; Fisher Scientific) was combined with 4 mL of 0.1 mg/mL β-LG. The mixture was allowed to incubate at 25 ± 1°C for a duration of 1 h. After incubation, 250 μL aliquots of the mixture was dispensed onto Nunc 96-well UV Transparent Microplates (Thermo Fisher Scientific), excited at 375 nm, and the emission was recorded between wavelengths of 400 and 650 nm with 5 nm increments. The spectral analysis was performed at 25 ± 1°C, and samples were analyzed in triplicate. As previously described by Kato and Nakai (1980), Nakai (1983), Li et al. (2007), Xiang et al. (2011), surface hydrophobicity was defined as the ratio of its extrinsic fluorescence to the protein concentration. The surface hydrophobicity of the samples was expressed as the ratio of the spectra obtained to the whey protein concentration.

FT-MIR Spectroscopic Measurements and Chemometric Analysis

The FT-MIR spectral data were acquired using a portable Agilent 4500 FTIR spectrometer (Santa Clara, CA) equipped with a triple reflection diamond crystal attenuated total reflectance (**ATR**) accessory and thermoelectrically cooled deuterated-triglycine sulfate (**DTGS**) detector. Spectra of untreated, thermally treated, and supercritically treated β-LG were recorded using MicroLab software (v. 5.1, Agilent Technologies, Santa Clara, CA) ranging from 4,000 to 700 cm^{-1} with a resolution of 8 cm^{-1}, and the spectra is the result of the average of 128 scans per sample. After each measurement, the diamond crystal was cleaned using 70% ethanol (Thermo Fisher). Background was performed per each measurement, and every sample was measured in triplicate.

Averaged FT-MIR spectral data were preprocessed using mean centering, normalization, and second derivative Savitzky-Golay (15-point window) using Pirouette 4.5 software (Infometrix, Bothell, WA). The FT-MIR spectra were preprocessed by transmission to absorbance (log[1/T]), and further transformed by standard normal variate, second derivative Savitzky-Golay (9-point window), and finally preprocessed by mean centering. Soft independent modeling of class analogy (**SIMCA**), a supervised classification technique based on principal components analysis (Vanden Branden and Hubert, 2005), was used to build a 2- and 3-class algorithm to discriminate untreated (class 1), thermal-treated (class 2), and processed using $ScCO_2$ (class 3). A 2-class model was used to compare effects of heat and $ScCO_2$ treatment to the untreated sample, as well as identifying differences between heat and $ScCO_2$ treatment. We then used a 3-class model to compare protein structure variations across the 3 sample sets. The SIMCA model was evaluated based on class projections, loadings, misclassifications, discriminating power, and interclass distances (Wang et al., 2015a). If the object is located within a restricted space of a training class, defined by its orthogonal and Mahalanobis

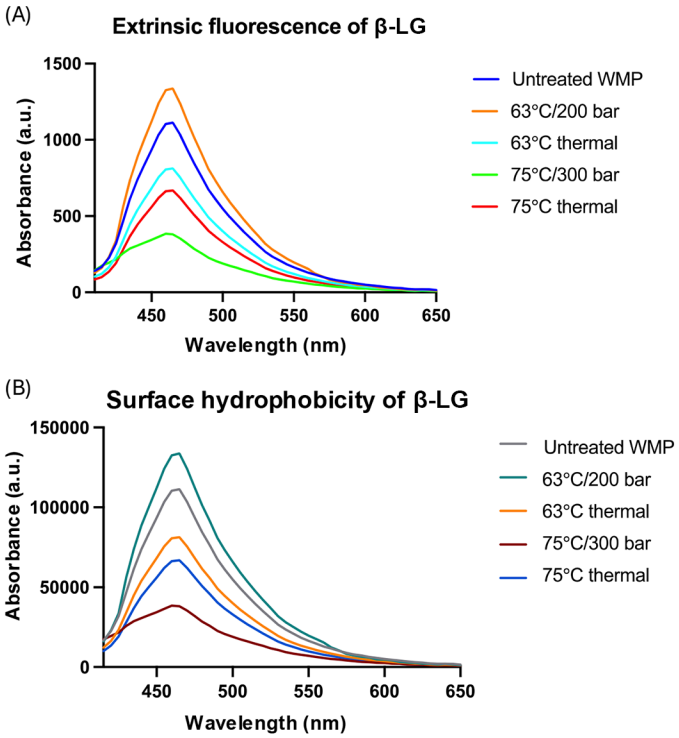

Figure 2. (A) Extent of protein unfolding determined by 8-anilino-1-naphthalenesulfonic acid binding and (B) surface hydrophobicity of β-LG isolated from whole milk powder under varied supercritical CO_2 and thermal treatment conditions. WMP = whole milk powder; a.u. = absorbance unit.

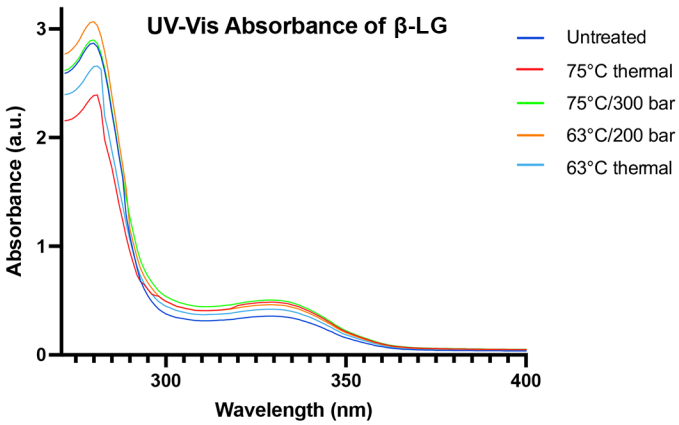

Figure 3. The UV-visible absorption spectra of β-LG isolated from whole milk powder under varied supercritical and thermal treatment conditions. a.u. = absorbance unit.

distances, then the object is assigned to that particular class (Custers et al., 2015).

Circular Dichroism Spectroscopy

Circular dichroism (**CD**) spectroscopy is a form of light absorbance spectroscopy that measures the difference in absorption of right and left circularly polarized light of a protein in solution. Mathematical treatment can be used to interpret changes in secondary structure. The effect of supercritical and thermal treatment on the secondary structure of β-LG was evaluated by means of CD spectroscopy. The β-LG solutions were prepared in ultrapure water (18 MΩ·cm) as a 0.35 mg/mL solution for far-UV analysis. The CD spectra was obtained at 25 ± 2°C using quartz cells (0.1 cm path length) and a Jasco J-815 spectropolarimeter (Jasco, Japan). Far-UV spectra covered 190 to 240 nm, with readings measured every 1 nm and a scan rate of 100 nm/min. Each spectrum was reported as an average of 3 scans. The secondary structure of β-LG was estimated using an online CD website (http://dichroweb.cryst.bbk.ac.uk). All spectra were corrected by subtracting the baseline and converting to mean residue ellipticity (deg·cm^2·dmol^{-1}) based on a mean AA residual weight of 114 (**MRW**; Divsalar et al., 2006). Spectral deconvolution was performed using the CONTIL (Provencher and Gloeckner, 1981) algorithm. Reference set used for this analysis was specific to wavelengths between 190 to 240 nm and were used from the suite of programs available at the online server DICHROWEB (http://dichroweb.cryst.bbk.ac.uk; Lobley et al., 2002; Whitmore and Wallace, 2008; Miles et al., 2021).

Statistical Analysis

All experiments were conducted with freshly prepared $ScCO_2$ processed samples. Results are reported as mean ± SD of triplicate measurements. Statistical analysis was performed using JMP Pro 15 (SAS Institute, Cary, NC) and GraphPad Prism (v9.0; GraphPad, San Diego, CA, https://www.graphpad.com/). Experiments were conducted and analyzed in triplicate unless indicated otherwise.

One-sample *t*-test was used to compare $ScCO_2$ and heat-treated samples with the untreated (control) sample. *P*-values <0.05 were considered to be significant.

RESULTS AND DISCUSSION

Purification of Proteins

The ß-LG from untreated WMP and samples treated under $ScCO_2$ and thermal conditions were isolated from WMP suspensions. The concentration of β-LG was estimated using a Pierce Coomassie (Bradford) Protein Assay kit (Thermo Fisher Scientific). A standard curve was prepared using BSA (Thermo Fisher Scientific) and β-LG (Thermo Fisher Scientific), with concentrations ranging

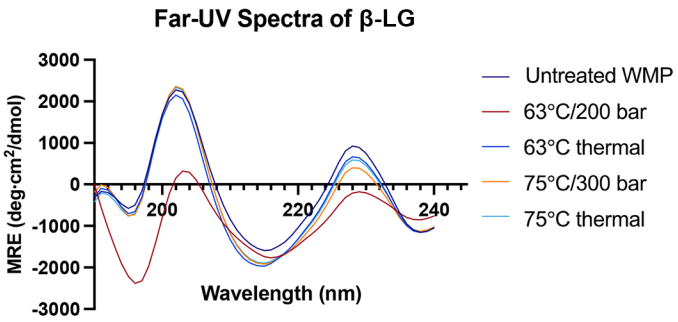

Figure 4. Far-UV circular dichroism spectra of β-LG isolated from whole milk powder under varied supercritical and thermal treatment conditions. WMP = whole milk powder; MRE = mean residual ellipticity.

Table 2. Percentage of different secondary structure components of β-LG—untreated, thermally treated, and under $ScCO_2$ conditions[1]

Sample	% Helix	% β-strands	% β-turns	% Random coils
Untreated	4.59 ± 0.16	36.00 ± 2.69	18.88 ± 1.12	40.54 ± 1.62
63°C/200 bar	5.78 ± 0.00*	31.78 ± 3.42*	18.31 ± 2.19*	44.17 ± 2.41*
63°C thermal	4.90 ± 0.00*	35.30 ± 2.32*	18.60 ± 0.00*	41.19 ± 1.26*
75°C/300 bar	5.03 ± 0.22*	34.62 ± 3.11*	18.12 ± 1.52*	42.18 ± 1.31*
75°C thermal	4.54 ± 0.18	35.64 ± 3.44	18.37 ± 1.27*	41.43 ± 2.53*

[1]Mean values of secondary structure composition of β-LG before and after heat and $ScCO_2$ treatment (±SD).

*Significant difference ($P < 0.05$) between that sample and the untreated sample.

between 5 to 30 µg/mL. The ratio of protein concentration obtained via the 2 standards was used to determine the purity of β-LG in the isolate and is reported in Table 1. To confirm the efficacy of this isolation, the fraction was also run through SDS-PAGE under reducing conditions. Analyses, as previously discussed in Venkatram et al. (2024), including ELISA, periodic staining, and proteomics analysis were repeated to verify if the isolate had reproducible results as when β-LG was a part of WMP.

Intrinsic Fluorescence

The Trp residues within proteins were chosen as intrinsic fluorescence probes to monitor structural modification of proteins upon heat and supercritical treatment. Figure 1 illustrates the intrinsic Trp fluorescence of β-LG with supercritical treatments at 63°C/200 bar, 75°C/300 bar, and thermal treatments at 63°C and 75°C, respectively. The untreated sample had an absorbance maximum of 980.46 absorbance units at 373 nm. Supercritical treatment at 63°C/200 bar led to a 2-nm blue shift (373–371 nm) in the emission wavelength, whereas treatment at 75°C/300 bar produced a 2-nm red shift (373–375 nm). In comparison to supercritical samples, both thermal controls produced a red shift of 2 nm, with a reduction in the maximum absorbance as the intensity of thermal treatment was increased. The observed red shifts that occurred in 3 of 4 treatment conditions indicate that the microenvironment around Trp residues was undergoing some kind of modification.

Previous studies by Manderson et al. (1998) and Moro et al. (2011) confirm protein unfolding resulting from partial protein denaturation, which caused a red shift on the fluorescence emission spectrum. Protein unfolding increases the exposure of the previously buried inner hydrophobic groups (aliphatic and aromatic AA residues), which can then easily be detected by fluorescence probes using appropriate aqueous solutions. This study confirmed that intrinsic fluorescence intensity of β-LG increased and the red shifts in the emission spectra are apparently due to the unfolding of the β-LG that resulted during heat and supercritical treatment. Such red shifts indicate a change in the polarity of the Trp environment, from a hydrophilic environment to a less hydrophilic environment, thus our observations indicate that β-LG might now be in a more hydrophobic environment (Elmnasser et al., 2008), which is consistent with our initial hypothesis about exposure of hydrophobic regions and also from our previous results where we detected the presence of capric acid bound to β-LG. Additionally, Kulmyrzaev and Dufour (2002) also discussed the effect of heat treatment on the potential red shift in the maximum intrinsic Trp intensity due to partial denaturation and formation of Maillard reaction products that we detected in our earlier sections. Another aspect of discussion is the emission quantum yields, which increased on $ScCO_2$ presence but decreased on thermal treatments.

These observations can be primarily attributed to changes in the conformation (Eftink, 1994; Andrade and Costa, 2002). The β-LG has 2 Trp residues, Trp_{19} and Trp_{61}. The Trp_{19} is located within the hydrophobic calyx comprised by the antiparallel β-strands, whereas Trp_{61} is in close proximity to the disulfide bond formed between Cys_{66} and Cys_{160} lying close to the protein surface (Papiz et al., 1986). Based on our observations and previously published literature, an increase in intensity quantum can be attributed to exposure of Trp residues to the exterior, which is predominant under $ScCO_2$ conditions due to its inherent hydrophobicity, whereas its reduction under thermal conditions could arise potentially due to aggregation of β-LG molecules.

The intrinsic fluorescence of supercritical samples was higher than the untreated sample, whereas dry heating diminished its intrinsic fluorescence. This result brings us to a conclusion that hydrophobic $ScCO_2$ treatment led to an unfolding of β-LG, exposing Trp residues to the exterior and thus increasing its intrin-

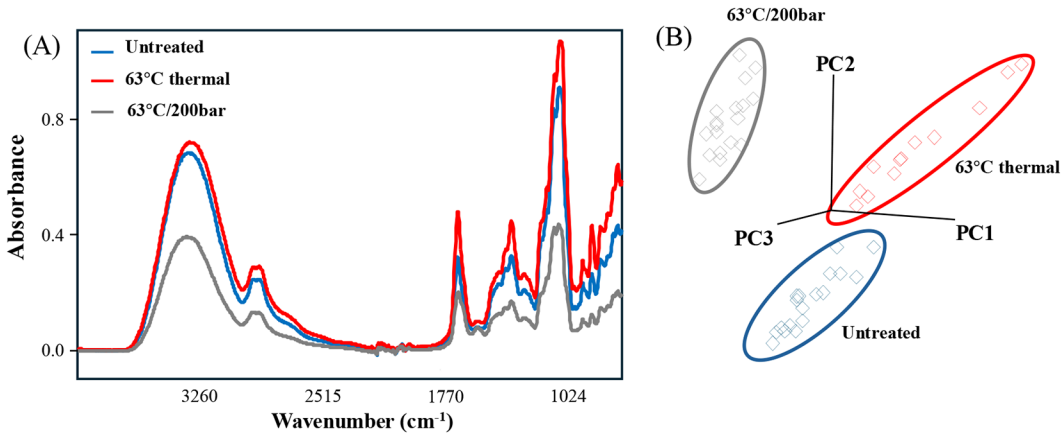

Figure 5. (A) Average attenuated total reflectance Fourier-transform mid infrared (ATR-FT-MIR) spectra acquired using portable mid-IR spectrometer and (B) soft independent modeling of class analogy (SIMCA) class projections of untreated β-LG, β-LG thermally treated at 63°C, and β-LG under supercritical CO_2 condition of 63°C/200 bar samples. PC = principal component.

sic fluorescence. Here, capric acid binding with β-LG produced a higher unfolding of the protein structure compared to lactosylation, as seen previously. This observation could also be due to stearic hindrance of lactose moieties and its ability to block Trp residues from energy absorption or emission. The intrinsic fluorescence of heat-treated β-LG decreased with increased heating temperature, indicating aggregation of protein molecules, thereby burying Trp residues present in β-LG. Thus, both heat treatment and $ScCO_2$ treatment produce conformational changes in the protein structure, the former leading to aggregation, whereas the latter leads to a higher extent of protein unfolding compared to the original (untreated) sample. This change highlights the unique denaturation mechanism of $ScCO_2$ compared to dry heating. Also, the red and blue shifts observed indicate the change in hydrophobicity of the protein molecule. Thermal treatments and $ScCO_2$ at 75°C/300 bar made the protein more hydrophobic (red shift), whereas treatment at 63°C/200 bar made the protein more hydrophilic (blue shift).

Extrinsic Fluorescence

The ANS is a chemical that specifically binds to the hydrophobic regions of proteins producing extrinsic fluorescence. The increase in extrinsic fluorescence generally indicates the exposure of previously buried hydrophobic regions to the environments or the loosening of protein folding (Chen et al., 2018). Thus, the fluorescence property of proteins is a unique property that allows us to probe the conformational changes of proteins caused by physical and chemical treatments (Yanjun et al., 2014).

Based on our observations illustrated in Figure 2, the extrinsic fluorescence of β-LG under treatment conditions of 63°C/200 bar was much higher compared to untreated β-LG, indicating the structure became looser, thereby allowing ANS molecules to enter to the protein's hydrophobic core. Additionally, β-LG binding with capric acid does also affect the overall extrinsic fluorescence. This observation is consistent with findings of Sponton et al. (2015), who studied binding properties between ovalbumin nanoparticles and linoleic acid and observed a 6- to 8-fold increase in surface hydrophobicity upon incorporation of linoleic acid molecules. Treatment at 75°C/300 bar produced a significant reduction in the surface hydrophobicity, implying that lactosylation could partially unfold the structure of β-LG and shield hydrophobic patches on the surface of β-LG molecule. This observation is consistent with the findings of Yang et al. (2017), who studied glycation of β-LG with mannose and Chen et al. (2016) with galactose. This result could also be attributed to the blocking of Lys, or Arg residues in the glycation conjugates because of the increasing hydrophilic groups by conjugation between carbohydrates and the ε-amino group of Lys during reaction, or both (Jiménez-Castaño et al., 2007; Corzo-Martínez et al., 2008). The reduction in the surface hydrophobicity of β-LG from thermal control samples was found to decrease, indicating protein aggregation. This aggregation protects the hydrophobic regions of the proteins. The partially denatured proteins with increased surface hydrophobicity might cause more extensive bonding and then reduce surface hydrophobicity of these proteins (Yanjun et al., 2014).

The $ScCO_2$ at 63°C/200 bar increased the overall extrinsic fluorescence and surface hydrophobicity of

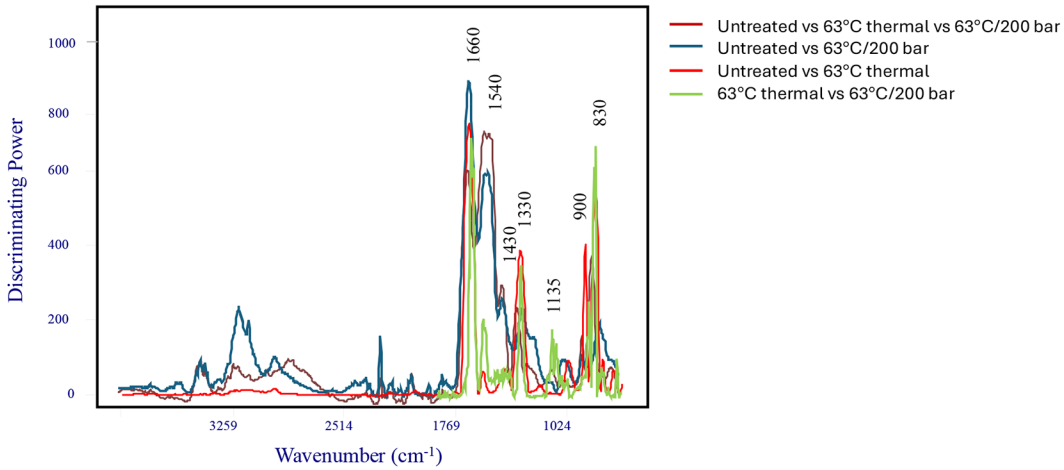

Figure 6. Soft independent modeling of class analogy (SIMCA) discriminating power based on the attenuated total reflectance-Fourier-transform mid infrared (ATR-FT-MIR) spectra of control, thermally, and supercritical CO_2-processed β-LG at 63°C acquired using portable mid-IR spectrometer. This figure is based on a 2-class SIMCA comparing 2 given sets of processing methods (untreated vs. $ScCO_2$ or untreated vs. thermal or thermal vs. $ScCO_2$) and also includes a 3-class SIMCA comparing the 3 samples (untreated vs. thermal vs. $ScCO_2$).

β-LG that is contributed both by protein unfolding and interaction with capric acid. Thereby exposure of buried hydrophobic residues and binding with a hydrophobic substance could increase the overall surface hydrophobicity. The drastic decrease in surface hydrophobicity under $ScCO_2$ conditions of 75°C/300 bar could be attributed to lactosylation and its blocking effect on hydrophobic patches, thereby restricting access of ANS to these regions. Both heat treatments produced a diminished extrinsic fluorescence, indicating aggregation which leads to burial of hydrophobic patches and close association of protein molecules, making them inaccessible to ANS. Thus, the 2 $ScCO_2$ treatments produced unique modifications to the structure of β-LG based primarily on its binding with capric acid or lactose. This observation was different from thermal controls, where slight lactosylation was indicated, although protein aggregation had a predominant effect on its structural characteristics.

UV-Visible Absorption Spectra

The UV-absorption spectroscopy is used to get the information about secondary (far-UV) and tertiary (near-UV) structural change of proteins. The chromophores of AA Trp, Try, and Phe showed specific electronic absorption bands in between 255 and 300 nm. The aromatic AA, specifically Trp, display a peak close to 280 nm.

As seen in Figure 3, the maximum absorbance was observed close to 280 nm, originating primarily from Trp. There was no apparent blue or red shift upon thermal or supercritical treatment. Another peak observed was observed close to 330 nm, which could be deduced to indicate the presence of sugars, as indicated in a previous study by Chevalier et al. (2001). This peak at 330 nm arising due to the presence of sugar residues was maximum for 75°C/300 bar, which agreed with previous studies that this condition produced the highest extent of lactosylation. The maximum absorbance of the untreated β-LG sample was 2.86 at 280 nm, 2.78 for the 75°C thermal sample, 2.89 for 75°C/300 bar, 2.65 for 63°C thermal sample, and 3.35 for 63°C/200 bar condition. This overall variation with respect to the peak intensity of Trp can be attributed to the change in conformation of β-LG (Al-Shabib et al., 2018). The increase in peak intensity at 280 nm for the 63°C/200 bar treatment could primarily be attributed to the presence of capric acid. Such a similar observation was also reported by Al-Shabib et al. (2018), who studied the binding of rutin with β-LG. The decrease in Trp maximum intensity could be partly attributed to aggregation of β-LG molecules, whose effects were predominant in both our thermal controls. Such a similar observation was also made by Zhong et al. (2012) and Liu et al. (2011), who observed a reduction in the UV absorption and attributed it to the aggregation of β-LG molecules, although their studies focused on the application of dynamic high pressure microfluidization.

The $ScCO_2$ treatment at 63°C/200 bar produced the highest changes in the protein secondary structure, whereas its effect at 75°C/300 bar was comparable to the untreated sample, indicating minimal changes. Heat treatments produced a lower maximum absorption than the untreated sample, with its effects pronounced at elevated operating temperatures. This result indicates

Table 3. Interclass distances generated from ß-LG isolated from whole milk powder under different processing conditions at 63°C using Fourier-transform mid infrared spectral data[1]

Sample	Untreated @4	63°C thermal @3	63°C/200 bar @5
Untreated	0.00	—	—
63°C thermal	6.43	0.00	—
63°C/200 bar	8.98	9.87	0.00

[1]Untreated @4 means 4 factors are used in soft independent modeling of class analogy (SIMCA) model. Thermal @3 means 3 factors used in the SIMCA model, and 63°C/200 bar @5 means 5 factors were used in the SIMCA model.

Table 4. Interclass distances generated from ß-LG isolated from whole milk powder under different processing conditions using 4500 series attenuated total reflectance midinfrared spectra spectrometer[1]

Sample	Untreated @5	75°C thermal @4	75°C/300 bar @5
Untreated	0.00	—	—
75°C thermal	2.87	0.00	—
75°C/300 bar	14.47	12.82	0.00

[1]Untreated@5 means 5 factors are used in soft independent modeling of class analogy (SIMCA) model. Thermal @4 means 4 factors, and 75°C/300bar @5 means 5 factors used in the SIMCA model, respectively.

that the environments around the AA residues were changing significantly.

CD

The far-UV spectra of untreated, thermally, and $ScCO_2$-treated β-LG are illustrated in Figure 4. As we know, β-LG is predominantly a β-sheet protein, consisting of 9 antiparallel β-strands and 1 major α-helix at the C-terminus of the molecule (Shibayama, 2008). The far-UV CD spectrum of native β-LG is typical of a protein with an antiparallel β-structure with a broad negative minimum at 215 nm, as has been reported by several authors (Mehraban et al., 2013; Mohammadi et al., 2015). Among the 5 samples, the spectra for 63°C/200 bar was found to be the most different from others with respect to peak intensity and wavelength. The 63°C/200 bar had a peak negative at 199 nm in comparison to other treatments which produced a peak negative in the 215 to 216 nm range. The extreme positive peak for all samples ranged between 208 to 210 nm. The variation in intensity and wavelength of peak maxima is a representation of the ß-strands, which is found to vary significantly in the 63°C/200 bar, with very small changes at other conditions compared to the untreated sample.

The percent secondary structure of untreated β-LG and under thermal and supercritical treatments were calculated by an online CD website (http://dichroweb.cryst.bbk.ac.uk).

The average secondary structure composition of untreated β-LG was 4.589% α-helix, 36% ß-strands, 18.878% ß-turns, and 40.544% random coils, which was similar to observations by Kanakis et al. (2013) and Li et al. (2020). As seen in Table 2, there were significant increases in the relative contents of α-helix when heated at 63°C and under both $ScCO_2$ treatments. This increase in the content of α-helix was comparable between the 75°C/300 bar sample and the 63°C thermal control, whereas the highest increase was observed under $ScCO_2$ conditions of 63°C/200 bar. At this condition, there was a significant reduction in the content of ß-strands and an increase in the relative content of random coils, these observations could be attributed to partial destabilization of β-LG conformation by binding of the capric acid within the hydrophobic pocket, located in the interior of the β-barrel. Although slight variations with respect to α-helix content were observed, the remaining treatments did not produce a significant variation in the content of other structural components. Considine et al. (2007) reported that the trough at 216 nm gradually broadened and deepened, accompanied by β-LG unfolding. As seen in Figure 4, this trough is seen to widen under all conditions compared to the untreated sample, and its effect is most pronounced at 63°C/200 bar, indicating a high extent of structural modifications. Zhong et al. (2015) studied the effect of nystose and fructofuranosyl nystose on the antigenicity of β-LG via glycation and observed an increase in the content of α-helix in the presence of 1^F-β-fructofuranosyl nystose, but this decreased upon glycation with nystose, indicating that the nature of sugar affects the secondary structure and conformation of β-LG. Our results agree with a previous report by Luo et al. (2022), who studied the Maillard reaction between β-LG and polydextrose and observed minimal changes on the secondary structure of β-LG via CD, however, significant changes in the tertiary structure were found using Trp fluorescence spectroscopy. Berino et al. (2019) studied the interaction of vitamin D3 with β-LG and concluded that this binding mainly affected the ß-sheets more than the α-helix, which is fairly consistent with our data, where the major changes in ß-strands were observed at 63°C/200 bar, where we observed an increased binding to capric acid.

In agreement with the observations from previous sections, $ScCO_2$ treatment at 63°C/200 bar produced the most variation in the secondary structure of β-LG, with a significant reduction in β-sheets and a simultaneous increase in random coils contributed primarily by the unfolding of the protein molecule and its interaction with capric acid.

FT-MIR Spectroscopy

The FT-MIR spectroscopy provides complementary information about changes in the structure of β-LG upon

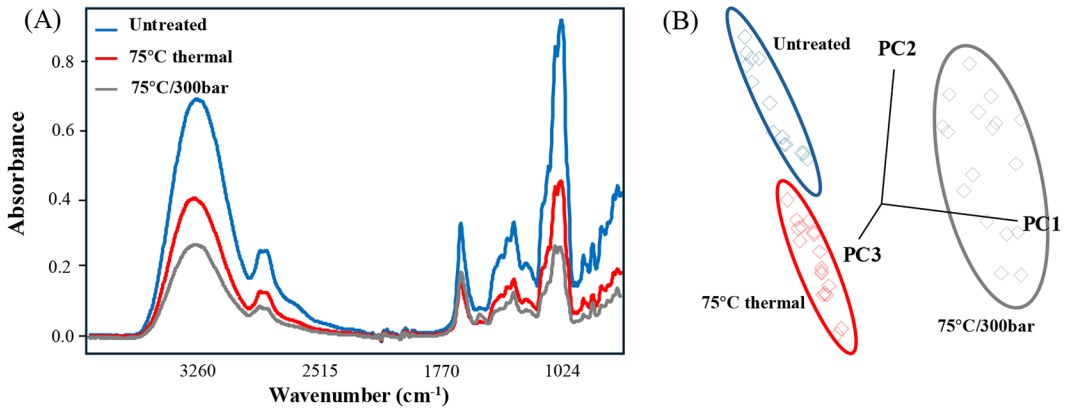

Figure 7. (A) Average attenuated total reflectance-Fourier-transform mid infrared (ATR-FT-MIR) spectra acquired using portable mid-IR spectrometer and (B) soft independent modeling of class analogy (SIMCA) classification plots untreated β-LG, β-LG thermally treated at 75°C, and β-LG under supercritical CO_2 condition of 75°C/300 bar samples.

heat and supercritical treatment. Figure 5 shows average spectra and SIMCA class projection plots for untreated β-LG, β-LG thermally treated at 63°C, and β-LG under supercritical CO_2 conditions of 63°C/200 bar.

The SIMCA class projection plots showed well-separated grouping of the samples analyzed in a 3-dimensional pattern. Clusters permitted tight clustering and clear differentiation between the 3 sample sets. Interclass distances (**ICD**) are Euclidian distances between centers of clusters, and above 3.0 are considered significant to identify 2 clusters as different classes (Dunn and Wold, 1995). The ICD values reported in Table 3 and as shown in Figure 5 varied from 6.40 to 9.87, showing significant chemical differences between the samples compared.

The discrimination power plot provides information about spectral patterns (specificity) and band intensity that are important for classification (discrimination or recognition). The major discriminating bands between the untreated, 63°C heat-treated, and 63°C/200 bar β-LG were observed at wavenumbers 1,660, 1,540, 1,430, 1,330, 1,135, 900, and 830 cm^{-1}. The absorbance at 1,660 cm^{-1} is attributed to the amide I band region, which is predominantly due to the C=O stretching vibration, with minor contributions from the out-of-phase CN stretching vibration, the CCN deformation, and the N–H in-plane bend (Barth, 2007). The discriminating band at 1,540 cm^{-1} belongs to amide II. The shoulder at the 1,540 cm^{-1} peak arises from the antisymmetric COO^- stretching vibrations of the carboxylate moiety of the AA side chain groups of glutamate and aspartate (Fabian and Vogel, 2002). The peak at 1,430 cm^{-1} corresponds to the stretching of C=O in the COO^- groups present in AA (Coates, 2006; Erukhimovitch et al., 2006). The discriminating wavenumbers at 1,330 cm^{-1} can be attributed to the amide III region, the in-phase combination of the N–H bending, and the C–N stretching vibration, with small contributions from the C–O in-plane bending and the C–C stretching vibration. The band at 1,135 cm^{-1} can be attributed to the C–H bending and the C–O stretching of fat (Chen and Irudayaraj, 1998). As per Kozłowicz et al. (2020), the absorbance at 900 cm^{-1} arises predominantly due to the stretching vibrations of C–O in the C–OH group and the stretching of C–C, and 830 cm^{-1} from the deformation vibrations of C–H and C–C groups in sugars. Figure 6 represents discriminating bands from comparisons of β-LG under temperature conditions of 63°C. Comparing the untreated and 63°C/200 bar sample, discriminations were predominantly due to the amide I, II, and III bands and corresponding to the COO^- group of AA indicative of a conformational change. This result matched with the fact that regular structures of protein will convert into more unfolded and random structures with increasing heating temperature (Stănciuc et al., 2012). Dry heating of WMP produced changes in the amide I and II regions, while also highlighting 2 bands at 900 and 830 cm^{-1}, indicative of sugar moiety presence. Thus, dry heating of WMP led to slight lactosylation. This is consistent with the findings of Bosman et al. (2021), who reported lactosylation of ß-LG when heated at 65°C with lactose for different time intervals. Comparing the 63°C/200 bar supercritical CO_2 sample with dry heating at 63°C, discriminating bands were in the amide I and III regions, with a shoulder at 1,135 cm^{-1} indicating the presence of a fatty acid moiety along with bands corresponding to the presence of sugars. Based on this comparison, we can conclude that fatty acid binding was important in discriminating the 63°C/200 bar condition from thermal heating, where lactosylation was also observed. This result agreed with our observations from proteomics analysis, wherein caprylation was observed in the untreated

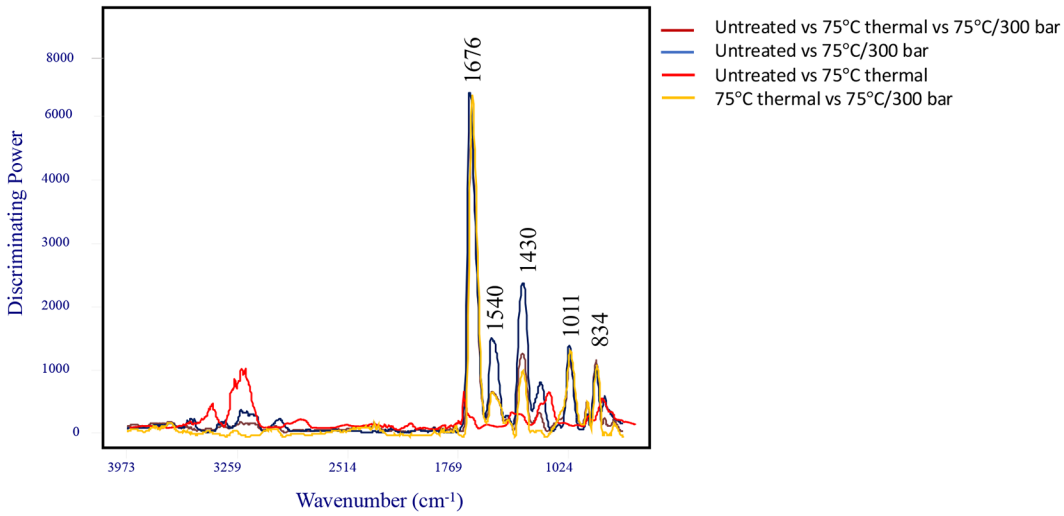

Figure 8. Soft independent modeling of class analogy (SIMCA) discriminating power based on the attenuated total reflectance-Fourier-transform mid infrared (ATR-FT-MIR) spectra of control, thermally, and supercritical CO_2-processed β-LG at 75°C acquired using portable mid-IR spectrometer. This figure is based on a 2-class SIMCA comparing 2 given sets of processing methods (untreated vs. $ScCO_2$ or untreated vs. thermal or thermal vs. $ScCO_2$) and also includes a 3-class SIMCA comparing the 3 samples (untreated vs. thermal vs. $ScCO_2$).

and supercritical CO_2 sample but not in the heat control. Finally, comparing the 3 samples, discriminating bands were associated with amide II region, from stretching of COO^- groups present in AA and deformation vibrations in C–H and C–C groups of sugars.

The average raw spectra and SIMCA class projection plots for untreated β-LG, β-LG thermally treated at 75°C, and β-LG under supercritical CO_2 conditions of 75°C/300 bar can be seen in Figure 7. The major discriminating bands between the untreated, 75°C heat-treated, and 75°C/300 bar β-LG, as seen in Figure 8, were observed at wavenumbers 1,676, 1,540, 1,430, 1,011, and 834 cm^{-1}. The bands at 1,676 and 1,540, and 1,430 cm^{-1} represent amide I and II regions (Barth, 2007). The peak at 1,430 cm^{-1} represents C=O stretching in the COO^- groups present in AA, whereas the peak at 1,011 cm^{-1} is due to the C–O and C–C stretching modes of sugars (Irudayaraj and Tewari, 2003), and at 834 cm^{-1} due to deformation vibrations of C–H and C–C groups in sugars. Comparing the untreated and 75°C/300 bar supercritical CO_2-treated sample, the major discriminating bands correspond to amide I and II regions, followed by a band at 1,430 cm^{-1} indicating protonation of the carboxylic group. Bands at 1,011 and 834 cm^{-1} indicate the presence of sugars. This result was consistent with our findings that lactosylation was highest at 75°C/300 bar, which had a pronounced effect on the antigenicity of β-LG. Very small discriminating bands were observed on comparing the untreated and 75°C thermal samples, indicating minor conformational changes.

The ICD is the critical parameter determined by measuring the distance between the geometric centers of 2 clusters (Albano et al., 1978), and this is conducted by the comparison of the F-statistic with a given CI, which is normally 95% (Meza-Márquez et al., 2010). The ICD greater than 3 are considered significant for the identification of data points as members of a group (Kvalheim and Karstang, 1992). As seen in Table 4 and Figure 7, the ICD between the untreated and thermally treated sample was 2.87, which concurs with the spectral findings that very small changes were produced under this treatment condition. All discriminating bands had a significance on comparing the 75°C/300 bar supercritical sample with the 75°C thermal sample. This indicates variations with respect to confirmation, as well as glycoprotein formation. Here the significant discriminating bands correspond to amide I region and COO^- protonation alongside vibrations involved within the sugar molecule (1,011 and 834 cm^{-1}). Finally, on comparing the 3 samples together, bands of differentiation were found in the amide I and II regions, with contribution arising from stretching of COO^- groups and vibrations contributed by sugar moieties, indicating that both structural conformational changes and glycoprotein formation were driving factors in producing these spectral variations.

As seen in the 2 comparisons under processing temperatures of 63°C and 75°C, thermal treatment mainly produced a significant variation with respect to the backbone structure of β-LG, as reflected in the amide I and III bands. However, $ScCO_2$ treatments not only modified the protein structure but also produced significant variations with regard to the functional groups of AA, as reflected in the amide II structure. Additionally, protonation of COO^- groups at wavenumber 1,430 cm^{-1} was observed as

a discriminating factor when compared against untreated and respective thermal controls. This observation could be attributed to interactions within functional groups of the constituent AA primarily via condensation and disulfide interactions, which can be attributed to protein aggregation, lactosylation, or caprylation.

Except for the comparison of thermal treatment at 75°C to untreated β-LG (2.87), all other treatments under thermal and supercritical conditions produced ICD higher than 3.0 when compared to differently treated β-LG samples. This result indicates that under varied effects of pressure and temperature, the structure of β-LG undergoes significant conformational changes, including aggregation, denaturation, lactosylation, or caprylation, which, in turn, would have an effect on its antigenicity (Zhong et al., 2012).

CONCLUSIONS

Secondary structure analysis of heat and supercritical CO_2-treated β-LG indicated conformational changes with exposure of hydrophobic groups, as reflected via fluorescence studies. Circular dichroism indicated changes in the secondary structure composition, with the highest changes encountered at 63°C/200 bar with a significant reduction of beta-sheet and formation of random coils, thereby concurring with our hypothesis of a unique denaturation mechanism. The FT-MIR studies indicated structural variations in the protein backbone, variations with regard to functional groups associated with AA residues, as well as the presence of sugar and fat moieties which identified lactosylation (75°C/300 bar) and caprylation (63°C/200 bar) as post translational modifications. This study helps correlate structure of an antigen (protein) to its recognition by a conjugate antibody. Evaluating IgE binding of $ScCO_2$-treated β-LG would help us to understand the role of secondary structure characteristics to the allergenicity of a protein, thus paving a path to produce hypoallergenic dairy products. Moreover, secondary structure components, primarily α-helices and ß-sheets, play an important role in functional properties, such as solubility, texture, emulsification, and gelling. Elucidating the effect of processing conditions on secondary structure of proteins would be key in producing novel dairy ingredients for food applications.

NOTES

We acknowledge the JT "Stubby" Parker Endowment in Dairy Foods at The Ohio State University for the financial support in carrying out this research (Columbus, OH). The authors thank Molly Davis (Food Science and Technology Department, The Ohio State University, Columbus, OH) for editing the manuscript. No human or animal subjects were used, so this analysis did not require approval by an Institutional Animal Care and Use Committee or Institutional Review Board. The authors have not stated any conflicts of interest.

Nonstandard abbreviations used: ANS = 8-anilino-1-naphthalenesulfonic acid; ATR = attenuated total reflectance; a.u. = absorbance unit; CD = circular dichroism; DTGS = deuterated-triglycine sulfate; FT-MIR = Fourier-transform mid infrared; ICD = interclass distances; MRE = mean residual ellipticity; MRW = mean residual weight; PC = principal component; SCF = supercritical fluid technology; SIMCA = soft independent modeling of class analogy; WMP = whole milk powder; WPI = whey protein isolate.

REFERENCES

Achouri, A., and J. I. Boye. 2013. Thermal processing, salt and high pressure treatment effects on molecular structure and antigenicity of sesame protein isolate. Food Res. Int. 53:240–251. https://doi.org/10.1016/j.foodres.2013.04.016.

Al-Shabib, N. A., J. M. Khan, A. Malik, M. A. Alsenaidy, M. T. Rehman, M. F. Al Ajmi, A. M. Alsenaidy, F. M. Husain, and R. H. Khan. 2018. Molecular insight into binding behavior of polyphenol (rutin) with beta lactoglobulin: Spectroscopic, molecular docking and MD simulation studies. J. Mol. Liq. 269:511–520. https://doi.org/10.1016/j.molliq.2018.07.122.

Albano, C., W. Dunn III, U. Edlund, E. Johansson, B. Nordén, M. Sjöström, and S. Wold. 1978. Four levels of pattern recognition. Anal. Chim. Acta 103:429–443. https://doi.org/10.1016/S0003-2670(01)83107-X.

Amaral, G. V., E. K. Silva, R. N. Cavalcanti, L. P. Cappato, J. T. Guimaraes, V. O. Alvarenga, E. A. Esmerino, J. B. Portela, A. S. Sant' Ana, M. Q. Freitas, M. C. Silva, R. S. L. Raices, M. A. A. Meireles, and A. G. Cruz. 2017. Dairy processing using supercritical carbon dioxide technology: Theoretical fundamentals, quality and safety aspects. Trends Food Sci. Technol. 64:94–101. https://doi.org/10.1016/j.tifs.2017.04.004.

Andrade, S. M., and S. M. B. Costa. 2002. Spectroscopic studies on the interaction of a water soluble porphyrin and two drug carrier proteins. Biophys. J. 82:1607–1619. https://doi.org/10.1016/S0006-3495(02)75512-4.

Barth, A. 2007. Infrared spectroscopy of proteins. Biochim. Biophys. Acta 1767:1073–1101. https://doi.org/10.1016/j.bbabio.2007.06.004.

Berino, R. P., G. D. Báez, G. A. Ballerini, E. E. Llopart, P. A. Busti, A. Moro, and N. J. Delorenzi. 2019. Interaction of vitamin D3 with beta-lactoglobulin at high vitamin/protein ratios: Characterization of size and surface charge of nanoparticles. Food Hydrocoll. 90:182–188. https://doi.org/10.1016/j.foodhyd.2018.11.027.

Bonnaillie, L. M., and P. M. Tomasula. 2012. Fractionation of whey protein isolate with supercritical carbon dioxide to produce enriched α-lactalbumin and β-lactoglobulin food ingredients. J. Agric. Food Chem. 60:5257–5266. https://doi.org/10.1021/jf3011036.

Bosman, G. P., S. Oliveira, P. J. Simons, J. Sastre Torano, G. W. Somsen, L. M. J. Knippels, R. Haselberg, R. J. Pieters, J. Garssen, and K. Knipping. 2021. Limited lactosylation of beta-lactoglobulin from cow's milk exerts strong influence on antigenicity and degranulation of mast cells. Nutrients 13:2041. https://doi.org/10.3390/nu13062041.

Chen, G., M. Miao, B. Jiang, J. Jin, O. H. Campanella, and B. Feng. 2018. Effects of high hydrostatic pressure on *Rhizopus chinensis* lipase: II. Intermediate states during unfolding. Innov. Food Sci. Emerg. Technol. 45:152–160. https://doi.org/10.1016/j.ifset.2017.08.018.

Chen, M., and J. Irudayaraj. 1998. Sampling technique for cheese analysis by FTIR spectroscopy. J. Food Sci. 63:96–99. https://doi.org/10.1111/j.1365-2621.1998.tb15684.x.

Chen, Y., Z. Tu, H. Wang, L. Zhang, X. Sha, J. Pang, P. Yang, G. Liu, and W. Yang. 2016. Glycation of β-lactoglobulin under dynamic high pressure microfluidization treatment: Effects on IgE-binding capacity and conformation. Food Res. Int. 89:882–888. https://doi.org/10.1016/j.foodres.2016.10.020.

Chevalier, F., J.-M. Chobert, M. Dalgalarrondo, and T. Haertlé. 2001. Characterization of the Maillard reaction products of β-lactoglobulin glucosylated in mild conditions. J. Food Biochem. 25:33–55. https://doi.org/10.1111/j.1745-4514.2001.tb00723.x.

Coates, J. 2006. Interpretation of Infrared Spectra, A Practical Approach. R. A. Meyers, ed. John Wiley & Sons, Ltd., Chichester, UK.

Considine, T., H. A. Patel, H. Singh, and L. K. Creamer. 2007. Influence of binding conjugated linoleic acid and myristic acid on the heat- and high-pressure-induced unfolding and aggregation of β-lactoglobulin B. Food Chem. 102:1270–1280. https://doi.org/10.1016/j.foodchem.2006.07.022.

Corzo-Martínez, M., F. J. Moreno, A. Olano, and M. Villamiel. 2008. Structural characterization of bovine β-lactoglobulin−galactose/tagatose Maillard complexes by electrophoretic, chromatographic, and spectroscopic methods. J. Agric. Food Chem. 56:4244–4252. https://doi.org/10.1021/jf7036714.

Crittenden, R. G., and L. E. Bennett. 2005. Cow's milk allergy: A complex disorder. J. Am. Coll. Nutr. 24(Suppl. 6):582S–591S. https://doi.org/10.1080/07315724.2005.10719507.

Custers, D., T. Cauwenbergh, J. L. Bothy, P. Courselle, J. O. De Beer, S. Apers, and E. Deconinck. 2015. ATR-FTIR spectroscopy and chemometrics: An interesting tool to discriminate and characterize counterfeit medicines. J. Pharm. Biomed. Anal. 112:181–189. https://doi.org/10.1016/j.jpba.2014.11.007.

Divsalar, A., A. A. Saboury, and A. A. Moosavi-Movahedi. 2006. Conformational and structural analysis of bovine β lactoglobulin-a upon interaction with Cr^{+3}. Protein J. 25:157–165. https://doi.org/10.1007/s10930-006-0007-3.

Dunn, W. J., Jr., and S. Wold. 1995. SIMCA pattern recognition and classification. Pages 179–193 in Chemometric Methods in Molecular Design. H. van de Waterbeemd, ed. VCH Verlagsgesellschaft mbH, New York.

Eftink, M. R. 1994. The use of fluorescence methods to monitor unfolding transitions in proteins. Biophys. J. 66:482–501. https://doi.org/10.1016/S0006-3495(94)80799-4.

Elmnasser, N., M. Dalgalarrondo, N. Orange, A. Bakhrouf, T. Haertlé, M. Federighi, and J.-M. Chobert. 2008. Effect of pulsed-light treatment on milk proteins and lipids. J. Agric. Food Chem. 56:1984–1991. https://doi.org/10.1021/jf0729964.

Erukhimovitch, V., M. Talyshinsky, Y. Souprun, and M. Huleihel. 2006. FTIR spectroscopy examination of leukemia patients plasma. Vib. Spectrosc. 40:40–46. https://doi.org/10.1016/j.vibspec.2005.06.004.

Fabian, H., and H. J. Vogel. (2002). Fourier transform infrared spectroscopy of calcium-binding proteins. Pages 57–74 in Methods in Molecular Biology. H. J. Vogel, ed. Springer, Totowa, NJ. https://doi.org/10.1385/1-59259-184-1:057.

Fox, K. K., V. H. Holsinger, L. P. Posati, and M. J. Pallansch. 1967. Separation of ß-lactoglobulin from other milk serum proteins by trichloroacetic acid 5. J. Dairy Sci. 50:1363–1367.

García-Cano, I., P.-W. Yeh, D. Rocha-Mendoza, and R. Jiménez-Flores. 2021. Supercritical CO_2 treatment reduces the antigenicity of buttermilk β-lactoglobulin and its inflammatory response in Caco-2 cells. JDS Commun. 2:1–6. https://doi.org/10.3168/jdsc.2020-0028.

Irudayaraj, J., and J. Tewari. 2003. Simultaneous monitoring of organic acids and sugars in fresh and processed apple juice by Fourier transform infrared—Attenuated total reflection spectroscopy. Appl. Spectrosc. 57:1599–1604. https://doi.org/10.1366/000370203322640242.

Jiménez-Castaño, L., M. Villamiel, and R. López-Fandiño. 2007. Glycosylation of individual whey proteins by Maillard reaction using dextran of different molecular mass. Food Hydrocoll. 21:433–443. https://doi.org/10.1016/j.foodhyd.2006.05.006.

Kanakis, C. D., P. A. Tarantilis, M. G. Polissiou, and H. A. Tajmir-Riahi. 2013. Probing the binding sites of resveratrol, genistein, and curcumin with milk β-lactoglobulin. J. Biomol. Struct. Dyn. 31:1455–1466. https://doi.org/10.1080/07391102.2012.742461.

Kato, A., and S. Nakai. 1980. Hydrophobicity determined by a fluorescence probe method and its correlation with surface properties of proteins. Biochim. Biophys. Acta Protein Struct. 624:13–20. https://doi.org/10.1016/0005-2795(80)90220-2.

Kozłowicz, K., R. Różyło, B. Gładyszewska, A. Matwijczuk, G. Gładyszewski, D. Chocyk, K. Samborska, J. Piekut, and M. Smolewska. 2020. Identification of sugars and phenolic compounds in honey powders with the use of GC–MS, FTIR spectroscopy, and x-ray diffraction. Sci. Rep. 10:16269. https://doi.org/10.1038/s41598-020-73306-7.

Kulmyrzaev, A., and É. Dufour. 2002. Determination of lactulose and furosine in milk using front-face fluorescence spectroscopy. Lait 82:725–735. https://doi.org/10.1051/lait:2002045.

Kvalheim, O. M., and T. V. Karstang. 1992. Chapter 7 SIMCA - Classification by means of disjoint cross validated principal components models. Pages 209–248 in Data Handling in Science and Technology. Elsevier.

Li, X., T. Dai, P. Hu, C. Zhang, J. Chen, C. Liu, and T. Li. 2020. Characterization the non-covalent interactions between beta lactoglobulin and selected phenolic acids. Food Hydrocoll. 105:105761. https://doi.org/10.1016/j.foodhyd.2020.105761.

Li, Y., Z. Chen, and H. Mo. 2007. Effects of pulsed electric fields on physicochemical properties of soybean protein isolates. Lebensm. Wiss. Technol. 40:1167–1175. https://doi.org/10.1016/j.lwt.2006.08.015.

Liu, C. M., J. Z. Zhong, W. Liu, Z. C. Tu, J. Wan, X. F. Cai, and X. Y. Song. 2011. Relationship between functional properties and aggregation changes of whey protein induced by high pressure microfluidization. J. Food Sci. 76:E341–E347. https://doi.org/10.1111/j.1750-3841.2011.02134.x.

Lobley, A., L. Whitmore, and B. A. Wallace. 2002. DICHROWEB: An interactive website for the analysis of protein secondary structure from circular dichroism spectra. Bioinformatics 18:211–212. https://doi.org/10.1093/bioinformatics/18.1.211.

Luo, Y., Y. Tu, F. Ren, and H. Zhang. 2022. Characterization and functional properties of Maillard reaction products of β-lactoglobulin and polydextrose. Food Chem. 377:131749. https://doi.org/10.1016/j.foodchem.2021.131749.

Manderson, G. A., M. J. Hardman, and L. K. Creamer. 1998. Effect of heat treatment on the conformation and aggregation of β-lactoglobulin A, B, and C. J. Agric. Food Chem. 46:5052–5061. https://doi.org/10.1021/jf980515y.

Mehraban, M. H., R. Yousefi, A. Taheri-Kafrani, F. Panahi, and A. Khalafi-Nezhad. 2013. Binding study of novel anti-diabetic pyrimidine fused heterocycles to β-lactoglobulin as a carrier protein. Colloids Surf. B Biointerfaces 112:374–379. https://doi.org/10.1016/j.colsurfb.2013.08.013.

Meng, X., Y. Bai, J. Gao, X. Li, and H. Chen. 2017. Effects of high hydrostatic pressure on the structure and potential allergenicity of the major allergen bovine β-lactoglobulin. Food Chem. 219:290–296. https://doi.org/10.1016/j.foodchem.2016.09.153.

Meza-Márquez, O. G., T. Gallardo-Velázquez, and G. Osorio-Revilla. 2010. Application of mid-infrared spectroscopy with multivariate analysis and soft independent modeling of class analogies (SIMCA) for the detection of adulterants in minced beef. Meat Sci. 86:511–519. https://doi.org/10.1016/j.meatsci.2010.05.044.

Miles, A. J., S. G. Ramalli, and B. A. Wallace. 2021. DichroWeb, a website for calculating protein secondary structure from circular dichroism spectroscopic data. Protein Sci. https://doi.org/10.1002/pro.4153.

Mohammadi, F., M. Sahihi, and A. K. Bordbar. 2015. Multispectroscopic and molecular modeling studies on the interaction of two curcuminoids with β-lactoglobulin. Spectrochim. Acta A Mol. Biomol. Spectrosc. 140:274–282. https://doi.org/10.1016/j.saa.2014.12.032.

Moro, A., G. D. Báez, P. A. Busti, G. A. Ballerini, and N. J. Delorenzi. 2011. Effects of heat-treated β-lactoglobulin and its aggregates on foaming properties. Food Hydrocoll. 25:1009–1015. https://doi.org/10.1016/j.foodhyd.2010.09.021.

Nakai, S. 1983. Structure-function relationships of food proteins: With an emphasis on the importance of protein hydrophobicity. J. Agric. Food Chem. 31:676–683. https://doi.org/10.1021/jf00118a001.

Papiz, M. Z., L. Sawyer, E. Eliopoulos, A. C. T. North, J. B. C. Findlay, R. Sivaprasadarao, T. A. Jones, M. E. Newcomer, and P. J. Kraulis. 1986. The structure of β-lactoglobulin and its similarity to plasma retinol-binding protein. Nature 324:383–385. https://doi.org/10.1038/324383a0.

Pedroza-Escobar, D., I. Castillo-Maldonado, T. González-Cortés, D. Delgadillo-Guzmán, P. Ruíz-Flores, J. H. S. Cruz, P. K. Espino-Silva, E. Flores-Loyola, A. Ramirez-Moreno, J. Avalos-Soto, M. Á. Téllez-López, S.-E. Velázquez-Gauna, R. García-Garza, R. D. A. P. Vertti, and C. Torres-León. 2023. Molecular bases of protein antigenicity and determinants of immunogenicity, anergy, and mitogenicity. Protein Pept. Lett. 30:719–733. https://doi.org/10.2174/0929866530666230907093339.

Provencher, S. W., and J. Gloeckner. 1981. Estimation of globular protein secondary structure from circular dichroism. Biochemistry 20:33–37. https://doi.org/10.1021/bi00504a006.

Singh, S. K., M. S. Pavan, S. P. N, and R. Kant. 2018. Applications of Super Critical Fluid Extraction in Milk and Dairy Industry: A Review. J. Food Process. Technol. 9. https://doi.org/10.4172/2157-7110.1000769.

Shibayama, N. 2008. Circular dichroism study on the early folding events of β-lactoglobulin entrapped in wet silica gels. FEBS Lett. 582:2668–2672. https://doi.org/10.1016/j.febslet.2008.06.047.

Sponton, O. E., A. A. Perez, C. R. Carrara, and L. G. Santiago. 2015. Linoleic acid binding properties of ovalbumin nanoparticles. Colloids Surf. B Biointerfaces 128:219–226. https://doi.org/10.1016/j.colsurfb.2015.01.037.

Stănciuc, N., I. Aprodu, G. Râpeanu, and G. Bahrim. 2012. Fluorescence spectroscopy and molecular modeling investigations on the thermally induced structural changes of bovine β-lactoglobulin. Innov. Food Sci. Emerg. Technol. 15:50–56. https://doi.org/10.1016/j.ifset.2012.03.001.

Vanden Branden, K., and M. Hubert. 2005. Robust classification in high dimensions based on the SIMCA method. Chemom. Intell. Lab. Syst. 79:10–21. https://doi.org/10.1016/j.chemolab.2005.03.002.

Venkatram, R., I. García-Cano, and R. Jiménez-Flores. 2024. Reduction in the antigenicity of beta-lactoglobulin in whole milk powder via supercritical CO_2 treatment. J. Dairy Sci. 107:4216–4234. https://doi.org/10.3168/jds.2023-24565.

Villa, C., J. Costa, M. B. B. P. Oliveira, and I. Mafra. 2018. Bovine milk allergens: A comprehensive review. Compr. Rev. Food Sci. Food Saf. 17:137–164. https://doi.org/10.1111/1541-4337.12318.

Wang, T., H. Xu, J. Han, E. Elbouchikhi, and M. E. H. Benbouzid. 2015a. Cascaded H-bridge multilevel inverter system fault diagnosis using a PCA and multiclass relevance vector machine approach. IEEE Trans. Power Electron. 30:7006–7018. https://doi.org/10.1109/TPEL.2015.2393373.

Wang, Z., J. Cao, and F. Meng. 2015b. Interactions between protein-like and humic-like components in dissolved organic matter revealed by fluorescence quenching. Water Res. 68:404–413. https://doi.org/10.1016/j.watres.2014.10.024.

Whitmore, L., and B. A. Wallace. 2008. Protein secondary structure analyses from circular dichroism spectroscopy: Methods and reference databases. Biopolymers 89:392–400. https://doi.org/10.1002/bip.20853.

Xiang, B. Y., M. O. Ngadi, L. A. Ochoa-Martinez, and M. V. Simpson. 2011. Pulsed electric field-induced structural modification of whey protein isolate. Food Bioprocess Technol. 4:1341–1348. https://doi.org/10.1007/s11947-009-0266-z.

Xu, D., F. Yuan, J. Jiang, X. Wang, Z. Hou, and Y. Gao. 2011. Structural and conformational modification of whey proteins induced by supercritical carbon dioxide. Innov. Food Sci. Emerg. Technol. 12:32–37. https://doi.org/10.1016/j.ifset.2010.10.001.

Yang, W., Z. Tu, H. Wang, L. Zhang, S. Xu, C. Niu, H. Yao, and I. A. Kaltashov. 2017. Mechanism of reduction in IgG and IgE binding of β-lactoglobulin induced by ultrasound pretreatment combined with dry-state glycation: A study using conventional spectrometry and high-resolution mass spectrometry. J. Agric. Food Chem. 65:8018–8027. https://doi.org/10.1021/acs.jafc.7b02842.

Yanjun, S., C. Jianhang, Z. Shuwen, L. Hongjuan, L. Jing, L. Lu, H. Uluko, S. Yanling, C. Wenming, G. Wupeng, and L. Jiaping. 2014. Effect of power ultrasound pre-treatment on the physical and functional properties of reconstituted milk protein concentrate. J. Food Eng. 124:11–18. https://doi.org/10.1016/j.jfoodeng.2013.09.013.

Yver, A. L., L. M. Bonnaillie, W. Yee, A. McAloon, and P. M. Tomasula. 2011. Fractionation of whey protein isolate with supercritical carbon dioxide—Process modeling and cost estimation. Int. J. Mol. Sci. 13:240–259. https://doi.org/10.3390/ijms13010240.

Zhong, J., Y. Tu, W. Liu, S. Luo, and C. Liu. 2015. Comparative study on the effects of nystose and fructofuranosyl nystose in the glycation reaction on the antigenicity and conformation of β-lactoglobulin. Food Chem. 188:658–663. https://doi.org/10.1016/j.foodchem.2015.05.015.

Zhong, J. Z., W. Liu, C. M. Liu, Q. H. Wang, T. Li, Z. C. Tu, S. J. Luo, X. F. Cai, and Y. J. Xu. 2012. Aggregation and conformational changes of bovine β-lactoglobulin subjected to dynamic high-pressure microfluidization in relation to antigenicity. J. Dairy Sci. 95:4237–4245. https://doi.org/10.3168/jds.2012-5333.